Radiology Case Reports 19 (2024) 1697–1701

Available online at www.sciencedirect.com

ScienceDirect

journal homepage: www.elsevier.com/locate/radcr

Case Report

Fatty-marrow transformation following radiotherapy for pancreatic cancer detected using dual-energy computed tomography: A case report ☆

Hirotaka Nakashima, MSc, RT[a,*], *Junji Mochizuki, MSc, RT*[b], *Fumihiro Sasaki, MSc, RT*[a], *Syunsuke Itaya, MSc, RT*[a], *Yuki Fukushima, MD, PhD*[c], *Takahiro Iida, MD, PhD*[d], *Yasuo Sakurai, MD, PhD*[e]

[a] *Department of Medical Radiation Technology, Teine Keijinkai Hospital, Sapporo, Japan*
[b] *Department of Radiology, Minamino Cardiovascular Hospital, Tokyo, Japan*
[c] *Department of Radiation oncology, Teine Keijinkai Hospital, Sapporo, Japan*
[d] *Department of Orthopedic, Teine Keijinkai Hospital, Sapporo, Japan*
[e] *Department of Diagnostic Radiology, Teine Keijinkai Hospital, Sapporo, Japan*

ARTICLE INFO

Article history:
Received 26 December 2023
Revised 26 January 2024
Accepted 29 January 2024

Keywords:
Dual-energy computed tomography
Fatty myelination
Radiation therapy
Fat/water ratio
Bone density

ABSTRACT

Bone damage, a late side effect of radiotherapy, occurs concurrently with the replacement of fat cells in the bone marrow, causing changes in bone composition. Changes in composition can affect bone quality and disease states, and reduced bone mass can reduce quality of life by increasing the risk of fractures. A 70-year-old woman presented to the orthopedic outpatient clinic with the chief complaint of lower-back pain. The patient reported no history of trauma but was in great pain and had difficulty walking. Since the patient had a history of pancreatic cancer, tumor-marker testing, bone scintigraphy, and dual-energy computed tomography were performed. Although the tumor-marker levels were normal, dual-energy computed tomography and bone scintigraphy revealed fresh compression fractures of the L1 and L3 vertebrae. In addition, dual-energy computed tomography material-discrimination analysis suggested high fat density in the L2 vertebral body. The patient had received approximately 30 Gy radiation to the L2 vertebral body for her pancreatic cancer, which resulted in fatty myelination in the bone. The diagnosis of fatty myelination is made on T1-weighted magnetic resonance images; however, diagnosis remains challenging because of the difficulty in assessing bone morphology on magnetic resonance images. More-

☆ Competing Interests: The authors declare that they have no known competing financial interests or personal relationships that could have appeared to influence the work reported in this paper.

* Corresponding author.
E-mail address: galileo_suusiki@yahoo.co.jp (H. Nakashima).

https://doi.org/10.1016/j.radcr.2024.01.085

over, some patients are not candidates for magnetic resonance imaging. Dual-energy computed tomography-based material-discrimination analysis can visually depict changes in the bone marrow, and is a valuable diagnostic tool owing to its simplicity.

Introduction

Radiotherapy is a common treatment for cancer [1,2]. Localized radiation is most commonly used for the treatment of malignancies of the prostate, pancreas, rectum, cervix, and endometrium. The effectiveness of radiotherapy, coupled with advances in treatment modalities, early detection, prevention, and cancer awareness, has dramatically improved patients' quality of life and reduced mortality. However, concerns regarding the effects of radiation on the adjacent tissues such as blood vessels and bone remain unresolved [3–5]. The changes observed in the bone and bone marrow (BM) after radiotherapy are similar to those in osteoporosis, including decreased trabecular bone mass, increased BM adiposity, increased BM CTX/TRAP5 levels, and prolonged fracture healing time [2]. Radiation also decreases the number of hematopoietic and skeletal stem cells in the BM [2,6]. These effects are dependent on the radiation dose, and radiotherapy decreased bone formation and promoted adipogenesis resulting in bone loss in a mouse model [7].

Intraosseous fat and fat sheaths can be diagnosed using T1-weighted magnetic resonance (MR) images, which show characteristic findings such as prolonged T1 relaxation time and high signal intensity with progression of the fat sheath [8,9]. Other imaging modalities include computed tomography (CT), which may show low absorption of X-rays associated with bone beam phenomena; however, CT may not provide sufficient data confirm the diagnosis [8,10] . Dual-energy CT (DECT) uses X-rays with 2 different energy levels to obtain two types of attenuation data. Elements at different energy levels have unique attenuation properties that allow the separation and quantification of materials provided that their elemental composition is known [11].

Additionally, a linear combination of any 2 substances can represent the attenuation coefficient of either substance, which is the principle of the material decomposition method [12,13].

The basic substance in the material decomposition method is called a substance base pair, and a variety of substances can be selected depending on the clinical problem [13]. Using this method, the fat components can be selectively imaged [11]. This allows clear visualization of the increased fat components, which is not possible with single-energy CT (SECT). This report illustrates the usefulness of DECT as a useful clinical diagnostic tool for radiotherapy-induced fat myelination.

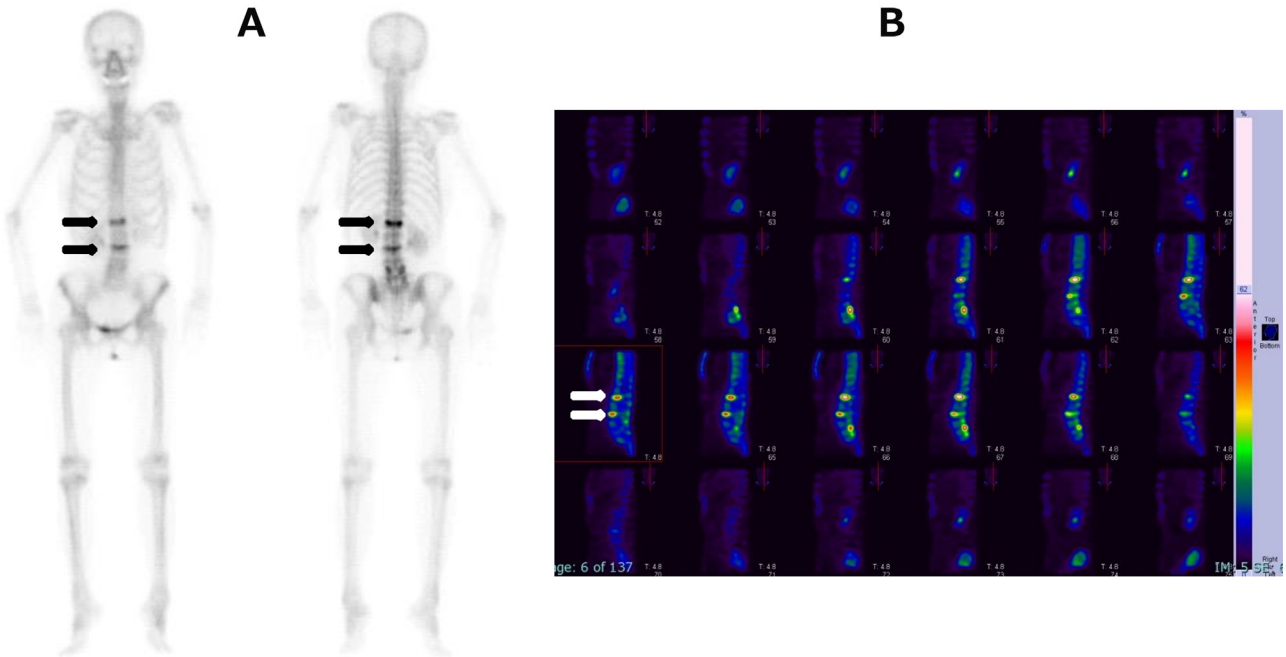

Fig. 1 – Bone scintigraphy findings. (A) frontal view. Whole-body bone scintigraphy shows accumulation of radiopharmaceuticals due to compression fractures at L1 and L3 (black arrow) (B) SPECT image shows similar findings (white arrow), with no abnormal accumulation observed at other sites.

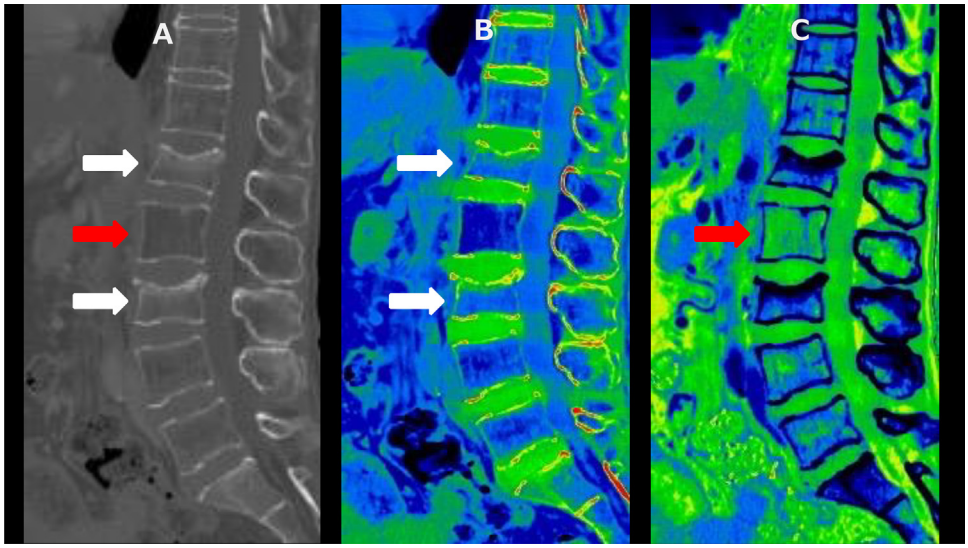

Fig. 2 – Sagittal DECT images showing fresh compression fractures in the L1 and L3 vertebrae. (A) 70 keV Bone image shows wedge-like changes (white arrow) and increased permeability (red arrow) suggesting a decrease in bone trabeculae. (B) Water/Calcium image shows increased water density in the vertebral body (white arrow) (C) Fat/Water image shows elevated fat in the vertebral body (red arrow) suggestive of fatty degeneration.

Case report

A 70-year-old woman presented to the orthopedic outpatient clinic with a chief complaint of lower-back pain. The patient reported no history of trauma but had persistent pain on sitting and standing, and she had difficulty walking because of the pain. The patient had undergone preoperative chemoradiotherapy (CRT) for pancreatic-head cancer 1 year prior to presentation. After CRT, tumor shrinkage was observed, and subtotal stomach-preserving pancreaticoduodenectomy was performed. The patient had no other significant medical history. Therefore, bone metastasis from pancreatic cancer was suspected, and tumor-marker testing, bone scintigraphy, and radiography were performed. Because the patient had difficulty with prolonged supine immobilization due to pain and claustrophobia, MR imaging was not feasible.

Tumor-marker levels were normal, but bone scintigraphy showed accumulation in the L1 and L3 vertebral bodies (Fig. 1). A compression fracture in the same area was suspected on standard CT, but no cancer metastasis was observed (Figs. 2 A and B). However, owing to defective bone trabeculae within the L2 vertebral body, a detailed evaluation was performed using DECT. Reconstruction of the material-degradation images for fat/water suggested fat densification in the L2 vertebral body (Fig. 2 C). Severe bone mineral density loss was observed only in the L2 vertebral body (Fig. 3).

The L1 and L3 vertebrae had osteoporotic compression fractures, and the L2 vertebral body was at high risk for fracture due to fatty myelination secondary to radiotherapy (Fig. 4). The patient was immediately started on medical therapy with a human anti-RANKL monoclonal antibody preparation, denosumab.

Discussion

Radiotherapy, even at minimal local doses, can cause adverse complications in adjacent organs, tissues, and blood vessels. In the bone, radiation exposure affects the structure of the minor column by increasing osteoclast activity and decreasing osteoblast activity, leading to a decrease in overall bone quantity and quality. Radiation-induced bone damage occurs concurrently with adipocyte infiltration into the BM, which may further affect bone quality and disease status. Hematopoietic cells also undergo radiation-induced apoptosis, which affects the skeleton in a variety of ways. Bone loss increases the risk of osteopenia, osteoporosis, osteonecrosis, and fractures and reduces the quality of life. Therefore, it is important to monitor intraosseous changes after radiotherapy to maintain the patient's quality of life. Fatty myelination can be diagnosed using T1-weighted MR images. The loss of T1 signal in vertebral bone marrow is linked to the replacement of fatty marrow by edema or cellular tissue. SECT shows a decreased signal in the vertebrae; however, confirming fatty myelination is difficult.

DECT uses X-rays with 2 different energy levels to differentiate the structures of human body components based on the attenuation characteristics associated with each energy level [11,12]. In the material-decomposition method, the material is selected according to the clinical problem.

Water and iodine are a pair of substances commonly used in clinical practice, and water-weighted images are similar to conventional CT images in that they represent the properties of water-like substances and are composed of low-atomic-number elements. Iodine-weighted images represent the properties of iodine-like substances (iodine and high-

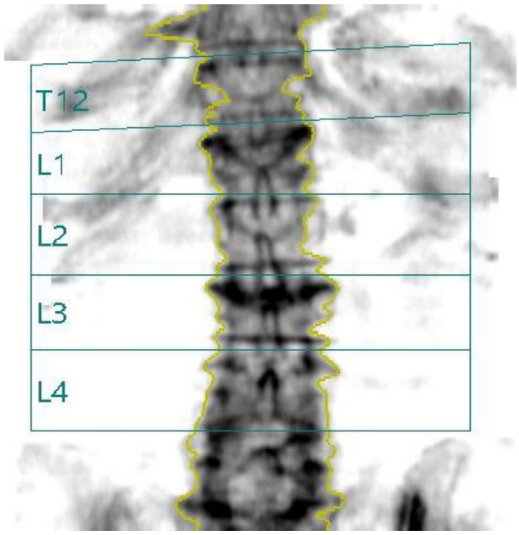

	BMD	Comparison to young Adult mean value		Comparison to age match value		BMC
	(g/c ㎡)	%	T score	%	Z score	g
T12	0.439 g/cm²	–	–	–	–	3.74 g
L1	0.516 g/cm²	50%	−3.6	72%	−1.4	4.93 g
L2	0.401 g/cm²	34%	−5.5	46%	−3.3	4.14 g
L3	0.596 g/cm²	50%	−4.2	68%	−2.0	6.87 g
L4	0.540 g/cm²	45%	−4.6	61%	−2.4	7.23 g
L1–L2	0.456 g/cm²	41%	−4.6	57%	−2.4	9.06 g
L1–L3	0.507 g/cm²	45%	−4.4	61%	−2.2	15.93 g
L1–L4	0.517 g/cm²	45%	−4.6	61%	−2.4	23.16 g
L2–L3	0.504 g/cm²	42%	−4.8	57%	−2.6	11.01 g
L2–L4	0.518 g/cm²	43%	−4.7	59%	−2.5	18.24 g
L3–L4	0.566 g/cm²	47%	−4.4	64%	−2.2	14.10 g

Fig. 3 – Results of the bone mineral density test using Dual Energy X-ray Absorptiometry The bone density is lower than the average in young adults and in the same age group, and osteoporosis is suspected. However, only the L2 vertebra shows a localized decrease in bone mineral density.

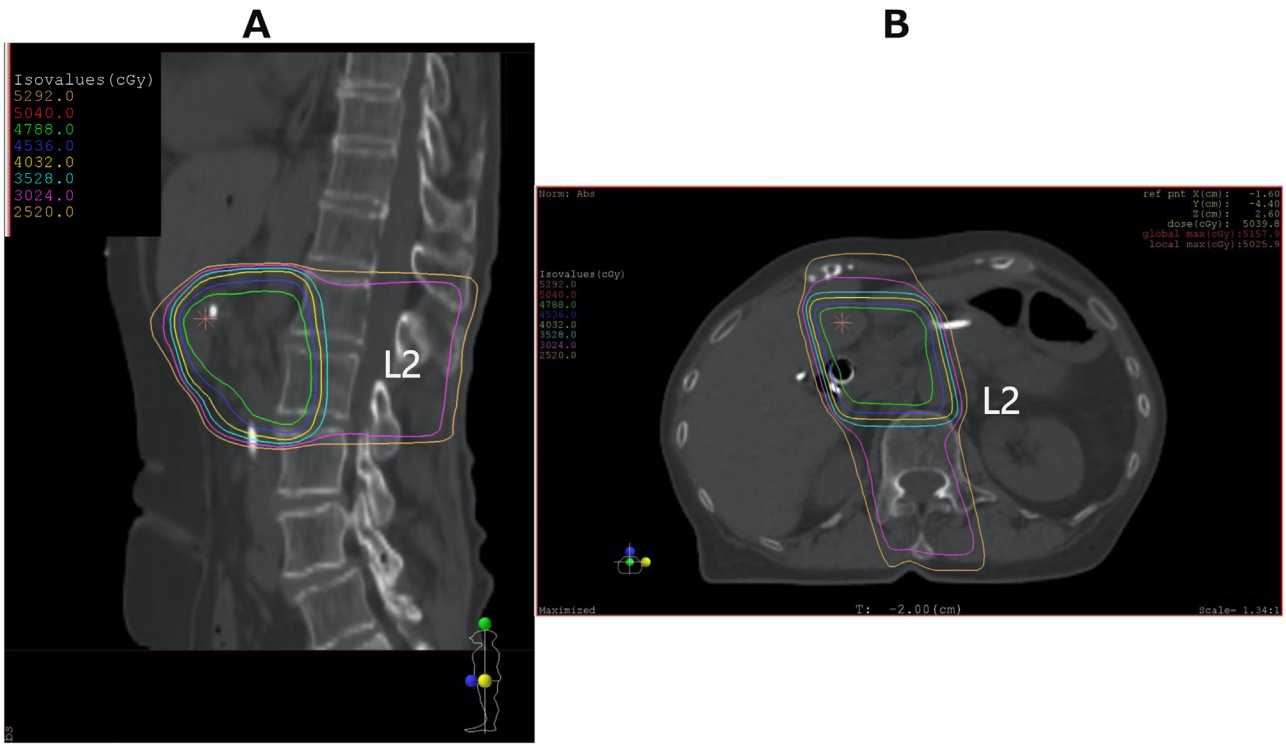

Fig. 4 – Dose distribution images (A, sagittal; B axial) of pancreatic-head cancer radiotherapy The radiotherapy dose distribution images show that 47.88 Gy was given in the green area, 35.28 Gy in the light blue area, and 25.20 Gy in the orange area. A high dose was given in front of the L2 vertebral body.

atomic-number metals). These images show the degree of iodine contrast and are used to diagnose conditions such as pulmonary embolism [14,15].

In recent years, virtual noncalcium imaging has been widely used in clinical practice to differentiate between bone edema and hematoma [16,17] and to evaluate the components of uric acid renal stones using effective atomic number imaging [18]. Fat-density images can be generated using fat and water as reference materials, and their usefulness in the diagnosis of fatty liver has been reported [19–21]. Furthermore, BM adipose-tissue imaging has validated the accuracy of fat detection [11].

In this case, fat density-weighted images showed fatty changes in the endosteal composition, which led to the diagnosis of a fatty medullary sheath.

DECT, similar to SECT, can evaluate cortical-bone morphology and is a good alternative for patients who cannot undergo MR imaging, such as this patient.

In conclusion, fatty myelin sheaths after radiotherapy increase bone fragility and the risk of fracture. Therefore, early detection of fatty components is important, and DECT can be a valuable diagnostic tool not only to evaluate the bone cortex but also to prevent the loss of quality of life due to compression fractures by identifying fatty components.

Patient consent

The patient provided permission to publish the details of his case and for the future use and publication of his images, at the time the images were obtained.

REFERENCES

[1] Bernier J, Hall EJ, Giaccia A. Radiation oncology: a century of achievements. Nat Rev Cancer 2004;4:737–47. doi:10.1038/nrc1451.

[2] Chandra A, Park SS, Pignolo RJ. Potential role of senescence in radiation-induced damage of the aged skeleton. Bone 2019;120:423–31. doi:10.1016/j.bone.2018.12.006.

[3] Green DE, Adler BJ, Chan ME, Lennon JJ, Acerbo AS, Miller LM, et al. Altered composition of bone as triggered by irradiation facilitates the rapid erosion of the matrix by both cellular and physicochemical processes. PLoS One 2013;8:e64952. doi:10.1371/journal.pone.0064952.

[4] Sparks RB, Crowe EA, Wong FC, Toohey RE, Siegel JA. Radiation dose distributions in normal tissue adjacent to tumors containing 131I or 90Y: the potential for toxicity. J Nucl Med 2002;43(8):1110–14.

[5] Curi MM, Cardoso CL, De Lima HG, Kowalski LP, Martins MD. Histopathologic and histomorphometric analysis of irradiation injury in bone and the surrounding soft tissues of the jaws. J Oral Maxillofac Surg 2016;74:190–9. doi:10.1016/j.joms.2015.07.009.

[6] Costa S, Reagan MR. Therapeutic irradiation: consequences for bone and bone marrow adipose tissue. Front Endocrinol 2019;10:587. doi:10.3389/fendo.2019.00587.

[7] Zou Q, Hong W, Zhou Y, Ding Q, Wang J, Jin W. Bone marrow stem cell dysfunction in radiation-induced abscopal bone loss. J Orthop Surg Res 2016;11:3. doi:10.1186/s13018-015-0339-9.

[8] Hochhegger B, Zanon M, Patel PP, Verma N, Eifer DA, Torres P, et al. The diagnostic value of magnetic resonance imaging compared to computed tomography in the evaluation of fat-containing thoracic lesions. Br J Radiol 2022;95:20220235. doi:10.1259/bjr.20220235.

[9] Unal E, Karaosmanoglu AD, Akata D, Ozmen MN, Karcaaltincaba M. Invisible fat on CT: making it visible by MRI. Diagn Interv Radiol 2016;22:133–40. doi:10.5152/dir.2015.15286.

[10] Beekman KM, Duque G, Corsi A, Tencerova M, Bisschop PH, Paccou J. Osteoporosis and bone marrow adipose tissue. Curr Osteoporos Rep 2023;21:45–55. doi:10.1007/s11914-022-00768-1.

[11] Yan SY, Yang YW, Jiang XY, Hu S, Su YY, Yao H, et al. Fat quantification: imaging methods and clinical applications in cancer. Eur J Radiol 2023;164:110851. doi:10.1016/j.ejrad.2023.110851.

[12] Mendonca PRS, Lamb P, Sahani DV. A flexible method for multi-material decomposition of dual-energy CT images. IEEE Trans Med Imaging 2014;33:99–116. doi:10.1109/TMI.2013.2281719.

[13] Patino M, Prochowski A, Agrawal MD, Simeone FJ, Gupta R, Hahn PF, et al. Material separation using dual-energy CT: current and emerging applications. Radiographics 2016;36:1087–105. doi:10.1148/rg.2016150220.

[14] Vlahos I, Jacobsen MC, Godoy MC, Stefanidis K, Layman RR. Dual-energy CT in pulmonary vascular disease. Br J Radiol 2022;95:20210699. doi:10.1259/bjr.20210699.

[15] Im DJ, Hur J, Han K, Suh YJ, Hong YJ, Lee H-J, et al. Prognostic value of dual-energy CT-based iodine quantification versus conventional CT in acute pulmonary embolism: a propensity-match analysis. Korean J Radiol 2020;21:1095. doi:10.3348/kjr.2019.0645.

[16] Akisato K, Nishihara R, Okazaki H, Masuda T, Hironobe A, Ishizaki H, et al. Dual-energy CT of material decomposition analysis for detection with bone marrow edema in patients with vertebral compression fractures. Acad Radiol 2020;27:227–32. doi:10.1016/j.acra.2019.02.015.

[17] Kaup M, Wichmann JL, Scholtz J-E, Beeres M, Kromen W, Albrecht MH, et al. Dual-energy CT–based display of bone marrow edema in osteoporotic vertebral compression fractures: impact on diagnostic accuracy of radiologists with varying levels of experience in correlation to MR imaging. Radiology 2016;280:510–19. doi:10.1148/radiol.2016150472.

[18] Li Z-X, Jiao G-L, Zhou S-M, Cheng ZY, Bashir S, Zhou Y. Evaluation of the chemical composition of nephrolithiasis using dual-energy CT in Southern Chinese gout patients. BMC Nephrol 2019;20:273. doi:10.1186/s12882-019-1441-8.

[19] Xu JJ, Boesen MR, Hansen SL, Ulriksen PS, Holm S, Lönn L, et al. Assessment of liver fat: Dual-energy CT versus conventional CT with and without contrast. Diagnostics 2022;12:708. doi:10.3390/diagnostics12030708.

[20] Beekman KM, Regenboog M, Nederveen AJ, Bravenboer N, Den Heijer M, Bisschop PH. Gender- and age-associated differences in bone marrow adipose tissue and bone marrow fat unsaturation throughout the skeleton, quantified using chemical shift encoding-based water–fat MRI. Front Endocrinol 2022;13:815835. doi:10.3389/fendo.2022.815835.

[21] Molwitz I, Leiderer M, Özden C, Yamamura J. Dual-energy computed tomography for fat quantification in the liver and bone marrow: a literature review. Rofo 2020;192:1137–53. doi:10.1055/a-1212-6017.